

Compact Model Training by Low-Rank Projection with Energy Transfer

Kailing Guo, *Member, IEEE*, Zhenquan Lin, Xiaofen Xing, *Member, IEEE*,
Fang Liu, *Member, IEEE*, Xiangmin Xu, *Senior Member, IEEE*

Abstract—Low-rankness plays an important role in traditional machine learning, but is not so popular in deep learning. Most previous low-rank network compression methods compress the networks by approximating pre-trained models and re-training. However, the optimal solution in the Euclidean space may be quite different from the one in the low-rank manifold. A well-pre-trained model is not a good initialization for the model with low-rank constraints. Thus, the performance of a low-rank compressed network degrades significantly. Compared to other network compression methods such as pruning, low-rank methods attracts less attention in recent years. In this paper, we devise a new training method, low-rank projection with energy transfer (LRPET), that trains low-rank compressed networks from scratch and achieves competitive performance. First, we propose to alternately perform stochastic gradient descent training and projection onto the low-rank manifold. Compared to re-training on the compact model, this enables full utilization of model capacity since solution space is relaxed back to Euclidean space after projection. Second, the matrix energy (the sum of squares of singular values) reduction caused by projection is compensated by energy transfer. We uniformly transfer the energy of the pruned singular values to the remaining ones. We theoretically show that energy transfer eases the trend of gradient vanishing caused by projection. Third, we propose batch normalization (BN) rectification to cut off its effect on the optimal low-rank approximation of the weight matrix, which further improves the performance. Comprehensive experiments on CIFAR-10 and ImageNet have justified that our method is superior to other low-rank compression methods and also outperforms recent state-of-the-art pruning methods. Our code is available at <https://github.com/BZQLin/LRPET>.

Index Terms—Network Compression, Low-Rank, Training Method.

I. INTRODUCTION

CONVOLUTIONAL neural networks (CNNs) have attained state-of-the-art performance in computer vision applications, like image classification [1], [2] and object detection [3]. However, such good performance is along with a large amount of storage and computing load, which restricts the deployment of CNN models on devices with limited resources. For instance, a ResNet-50 model needs roughly 4G FLOPs (floating-point operations per second) to categorize a color image with 224×224 pixels. Network compression is one kind

of typical methods for handling redundant or insignificant network components. Network compression includes low-rank decomposition [4]–[7], network pruning (sparsity) [8]–[10], parameter quantization [11], knowledge distillation [12], etc. Among them, low-rankness and sparsity are important properties for analyzing the intrinsic structure of data in traditional machine learning [13]–[18]. However, when things come to network compression, low-rankness is overlooked by researchers compared to the popularity of pruning. Low-rankness and sparsity respectively capture the global and local information of data. Both of them should be important for network compression. In this paper, we investigate the obstacles to applying low-rankness to network compression and propose a training method to tackle these problems.

For low-rank approximation (LRA) methods [19], reconstruction error may be accumulated layer by layer and degrade the performance even after fine-tuning. Since low-rank decomposed network and the original network are not of the same solution space, mimicking the original network is not the optimal choice. Training low-rank compact network from scratch seems more appealing. However, it is a great challenge to achieve satisfactory results. Low-rank network compression factorizes a big weight matrix into the product of small matrices, and thus the network becomes deeper by changing a layer into several consecutive small layers. In general, training a deeper network is harder. Trained rank pruning (TRP) [20] avoids training deeper network by performing low-rank projection (LRP) and training alternatively, which preserves and optimizes all parameters of the original network in the low-rank form. However, TRP needs computing singular value decomposition (SVD) at every iteration to guarantee its performance and is very time-consuming. SVD training [21] forces the factorized matrices in an SVD form with orthogonal and sparsity regularization to ease the training. However, a low-rank network’s capacity is limited compared with the original full-rank network, which makes it challenging to achieve comparable performance. Batch normalization (BN) is popular in modern networks and affects the optimal LRA of the weight matrix. However, BN’s effect has not been studied in previous low-rank network compression methods.

In this paper, we devise an efficient training method, low-rank projection with energy transfer (LRPET), that trains low-rank compressed networks from scratch and achieves competitive performance. Fig. 1 illustrates the procedure of LRPET. We propose to alternately perform stochastic gradient descent training and project onto the low-rank manifold with matrix energy (the sum of squares of singular values) transfer

Corresponding author: Xiangmin Xu.

Kailing Guo and Xiangmin Xu are with South China University of Technology, Guangzhou 510640, China, and with the Pazhou Lab, Guangzhou 510330, China (email: guokl@scut.edu.cn; xmxu@scut.edu.cn). Zhenquan Lin, and Xiaofen Xing are with South China University of Technology, Guangzhou 510640, China (email: zhenquan_lin@163.com; xfxing@scut.edu.cn). Fang Liu is with Guangdong University of Finance, Guangzhou 510521, China (e-mail: 47-032@gduf.edu.cn).

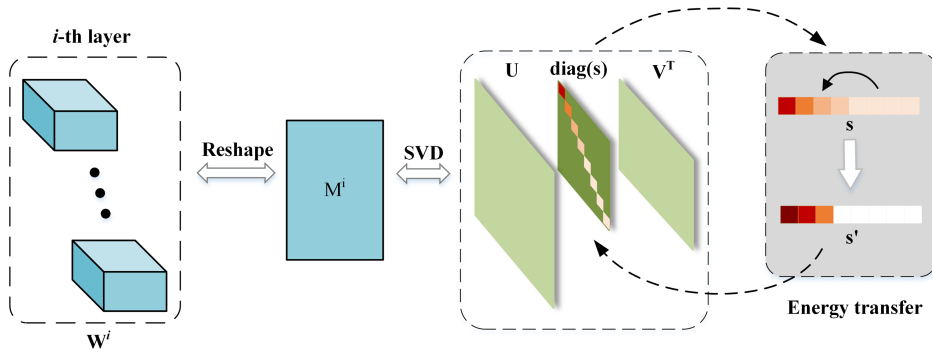


Fig. 1: An illustration of the procedure of energy transfer

to compensate energy reduction caused by projection. Our contributions are summarized as follows:

- LRP during training will result in gradient vanishing. Through theoretical analysis, we find that this is a new problem caused by training method rather than the traditional gradient vanishing caused by network structure. We discover and solve this problem with LRPET.
- Energy transfer is critical for training efficiency. To achieve good performance, TRP needs LRP for every iteration. With energy transfer, LRPET only needs to apply LRP once for every epoch, which is very efficient.
- To the best of our knowledge, LRPET is the first method to deal with BN's effect in low-rank network compression. By merging the linear transformation of BN into network weights, LRPET is compatible with BN and improves the final performance.

Our method is exciting since we show that low-rankness has the potential to achieve comparable performance to sparsity in such a simple way, which is overlooked in the community of network compression. We conduct a lot of experiments on the image classification task. The results show that our proposed method is effective and suitable for different networks (ResNet [1], VGGNet [22] and GoogLeNet [23]) on benchmark datasets (CIFAR-10 [24] and ImageNet [2]).

This paper is organized as follows. The related work is briefly reviewed in Section II. Section III describes the details of the proposed LRPET method. Section IV presents experimental results, and Section V concludes the paper.

II. RELATED WORKS

A. Low-Rank Decomposition

Low-rank decomposition methods decompose the weight matrix/tensor of a layer into several small matrices/tensors to reduce storage and computation cost. They can be divided into LRA and training low-rank networks from scratch.

1) *Low-Rank Approximation*: LRA methods compress the networks by approximating pre-trained models and re-training. Lebedev et al. [25] decompose the 4-D convolution kernel tensor into the sum of rank-one tensors and replace the original convolutional layer with a sequence of four convolutional layers with small kernels. However, too many layers make the gradients prone to gradient explosion/vanishing, and the re-training process needs careful design. Later works [6], [19]

reshape the 4-D tensor into a 2-D matrix and decompose the matrix into two small matrices, which results in two consecutive layers. Jaderberg et al. [19] construct a low rank basis of rank-1 filters in the spatial domain by minimizing weight matrix reconstruction error and get two consecutive layers with convolutional kernel sizes of $1 \times h$ and $w \times 1$. Zhang et al. [6] reconstruct linear or non-linear response with an approximate low-rank subspace, which actually divides a layer into two consecutive layers with convolution kernel sizes $w \times h$ and 1×1 . The performance of LRA alone may be unsatisfactory in practice, so recent works [26], [27] improve LRA by combining with other methods. Lin et al. [26] retrain the low-rank compression network through knowledge transfer and distillation. Collaborative compression (CC) [27] simultaneously learning the model sparsity and low-rankness to joints channel pruning and tensor decomposition. However, combining methods usually introduce extra computation cost.

For the LRA methods, decomposing the pre-trained network may result in a significant loss of accuracy, and the network needs retraining to recover the performance as much as possible. A well-pre-trained model is not a good initialization for the model with low-rank constraints. So some works try to obtain low-rank networks directly by training from scratch.

2) *Training From Scratch*: Training from scratch methods usually use regularization to guide the training process to learn low-rank network structure. Wen et al. [4] train neural networks toward lower-rank space by enforcing filters to become closer with a forced regularization motivated by physics. TRP [20] alternates performing LRP and training, which maintains the capacity of the original network while imposing low-rank constraints. However, they apply LRP according to a pre-defined energy pruning ratio, which makes each layer's rank varies and destabilizes the training process. Although TRP argues that their method does not cause the problem of gradient vanishing, we theoretically find that the gradient vanishing still exists. In this paper, we propose energy transfer to ease this problem and improve the performance. To guarantee the performance, TRP adds nuclear norm regularization, whose optimization needs time-consuming SVD at each iteration. To avoid SVD's inefficiency during training, SVD training [21] first decomposes each layer into the form of its full-rank SVD, and then performs training on the decomposed weight matrices. They use orthogonality and sparsity regularization

to keep the singular vector matrices close to unitary matrices and sparsify the singular values. To promote the performance of low-rank networks, Alvarez et al. [28] combine sparse group Lasso regularizer and nuclear norm-based low-rank regularizer, which encourages each layer’s weight matrix to be filter-wise sparse and low-rank. However, multiple regularizers require multiple trade-off hyperparameters, which are hard to tune. Adding regularizer means implicit constraint, and thus it is difficult to determine the compression rate before training. Note that a BN layer can be absorbed into the previous convolutional layer by modifying its weights after training and this will affect the optimal LRA of the weight matrix but has not been studied in previous low-rank network compression methods. In contrast, our LRPET is compatible with BN by applying LRP to the modified weight matrix that absorbs BN’s parameter, and this effectively improves the performance.

B. Network Pruning

Network pruning, which is orthogonal to low-rank decomposition, aims to remove the redundant or unimportant parts of the neural network. Non-structured pruning [8] is to prune specific weight elements in the network and requires complex hardware and/or software. Structured pruning [29] directly cuts off the filters or blocks in the network, which is easy to implement and is popular in recent researches [30], [31].

Li et al. [32] removes whole filters with their connecting feature maps according to ℓ_1 -norm. Channel pruning [33] and ThiNet [34] prune the whole filters by minimizing layer output reconstruction error with different selection strategy: channel pruning uses LASSO regression while ThinNet adopts greedy algorithm. Different from the above methods that prune filters by only considering the statistics of an individual layer or two consecutive layers, Yu et al. [31] minimize the reconstruction error of important responses in the final response layer and propagate the importance scores of final responses to every filter in the network for pruning. Considering that a smaller scaling parameter of BN layer indicates that the corresponding convolution filter’s effect is more negligible, Liu et al. [35] imposes ℓ_1 regularization on the scaling factors in BN, and channels with small scaling factors in BN layers are pruned. To avoid training inefficiency, HRank [36] investigates the rank of feature maps and proposes a new pruning criterion that prunes filters with low-rank feature maps. However, these methods require fine-tuning to restore performance.

Soft Filter Pruning (SFP) [30] train pruned networks from scratch by alternatively pruning with ℓ_2 norm and reconstructing the pruned filters from training. This soft manner can maintain the model capacity and avoid fine-tuning. Learning filter pruning criteria (LFPC) [37] develops a differentiable sampler to select pruning different criteria in pre-determined candidates for different layers. Instead of pre-determining the pruning criterion, Lin et al. [38] introduce a soft mask with sparsity regularization and generative adversarial learning (GAL) to select the pruned parts. Deep compression with reinforcement learning (DECORE) [39] automates the network compression process by assigning an agent to each channel along with a light policy gradient method to learn which

neurons or channels to be kept or removed. Fire together wire together (FTWT) [40] dynamically prune the network with a self-supervised binary classification module to predict a mask to process k filters in a layer based on the activation of its previous layer, which results in sample-wise adaptive pruned network structure. These methods benefit from the recently developed learning techniques, but at the same time increase the complexity of the training process.

III. LOW-RANK PROJECTION WITH ENERGY TRANSFER

A deep neural network composed of L layers is to successively compute the features $\mathbf{x}^l = \phi(\mathbf{W}^l \mathbf{x}^{l-1} + \mathbf{b}^l) \in \mathbb{R}^{N_l} \forall l = 1, 2, \dots, L$, where $\mathbf{x}^{l-1} \in \mathbb{R}^{N_{l-1}}$ is the input feature of the l^{th} layer, $\phi(\cdot)$ is element-wise nonlinear activation function, and $\mathbf{W}^l \in \mathbb{R}^{N_l \times N_{l-1}}$ and $\mathbf{b}^l \in \mathbb{R}^{N_l}$ are learnable weight matrix and bias vector, respectively. Note that through reshaping weight and input tensors into matrices in a proper way, convolution can be implemented by matrix multiplication. Thus, we use a weight matrix to denote either full connection or convolution. Although the input and output need reshape operation, we ignore them in the formulation for simplification since this does not affect the analysis in this paper. Suppose the final composition function of all layers is $f(\mathbf{x}; \Theta)$, where $\Theta = \{\mathbf{W}^l, \mathbf{b}^l | l = 1, 2, \dots, L\}$ denotes the set of learnable parameters. Given the training dataset $D = \{(\mathbf{x}_i, \mathbf{y}_i)\}_{i=1}^M$ composed of M samples with inputs $\mathbf{x}_i \in \mathbb{R}^{N_0}$ and outputs $\mathbf{y}_i \in \mathbb{R}^{N_y}$, and the loss function $\mathcal{L}(\mathbf{y}, f(\mathbf{x}; \Theta))$, the optimization objective function of an ordinary deep neural network is given by $\min_{\Theta} \mathbb{E}_{(\mathbf{x}, \mathbf{y}) \in D} [\mathcal{L}(\mathbf{y}, f(\mathbf{x}; \Theta))]$.

A. Low-Rank Projection

A low-rank matrix can be factorized into the product of two small matrices to save parameters and computation cost in matrix multiplication. Thus, learning low-rank weight matrices for each layer can compress the networks. Previous low-rank compression methods [5], [6] usually need pre-training, decomposition, and re-training to achieve this goal, which is time-consuming. The optimal solution lies in the low-rank manifold may be quite different from the one in the Euclidean space, and thus the pre-trained model is hard to guarantee good initialization for low-rank matrices. In this paper, we propose a training from scratch method to learn low-rank compressed models. The problem is formulated as follows:

$$\begin{aligned} \min_{\Theta} \mathbb{E}_{(\mathbf{x}, \mathbf{y}) \in D} [\mathcal{L}(\mathbf{y}, f(\mathbf{x}; \Theta))] \\ \text{s.t. } \mathbf{W}^l \in \Omega_{r_l}^{N_l, N_{l-1}} \forall l \in \{1, 2, \dots, L\}, \end{aligned} \quad (1)$$

where $\Omega_{r_l}^{N_l, N_{l-1}}$ stands for the manifold of rank- r_l matrices with the size of $N_l \times N_{l-1}$.

Intuitively, this problem can be solved by projected stochastic gradient descent (SGD), i.e., one step SGD update followed by projection onto the corresponding low-rank manifold. Since the operation for each layer is the same, we respectively simplify \mathbf{W}^l and $\Omega_{r_l}^{N_l, N_{l-1}}$ to \mathbf{W} and Ω_r in the follow-

ing. According to Eckart-Young theorem [41], the projection $\mathcal{P}_{\Omega_r}(\mathbf{W}) = \arg \min_{\hat{\mathbf{W}} \in \Omega_r} \|\hat{\mathbf{W}} - \mathbf{W}\|_F^2$ can be computed by

$$\mathcal{P}_{\Omega_r}(\mathbf{W}) = \sum_{i=1}^r s_i \mathbf{u}_i \mathbf{v}_i^T, \quad (2)$$

where s_i is the i^{th} largest singular value of \mathbf{W} , \mathbf{u}_i and \mathbf{v}_i are the corresponding singular vectors of \mathbf{U} and \mathbf{V} in the SVD $\mathbf{W} = \mathbf{U}\mathbf{S}\mathbf{V}^T$. However, applying SVD for \mathbf{W} after every iteration is time-consuming. Instead, we use a variant of projected SGD that projects \mathbf{W} onto Ω_r after a certain number of iterations, which does not increase too much training time.

B. Energy Transfer

LRP is a non-expansive operator that will reduce not only the Frobenius norm of the weight matrix but also the norm of the gradient of the corresponding feature map when back propagation. The subscripts “ $1:r, :$ ” and “ $:, 1:r$ ” denote the first r rows and the first r columns of the matrix, respectively. \mathbf{U}_\perp denotes the orthogonal complement of $\mathbf{U}_{:,1:r}^T$, i.e., the remainder columns of \mathbf{U} . LRP can also be computed by

$$\mathcal{P}_{\Omega_r}(\mathbf{W}) = \mathbf{U}_{:,1:r} \mathbf{U}_{:,1:r}^T \mathbf{W} = \mathbf{W} \mathbf{V}_{:,1:r} \mathbf{V}_{:,1:r}^T. \quad (3)$$

Then, we have

$$\begin{aligned} \|\mathcal{P}_{\Omega_r}(\mathbf{W})\|_F^2 &= \|\mathbf{U}_{:,1:r} \mathbf{U}_{:,1:r}^T [\mathbf{U}_{:,1:r}, \mathbf{U}_\perp] \mathbf{S} \mathbf{V}^T\|_F^2 \\ &= \|[\mathbf{U}_{:,1:r}, \mathbf{0}] \mathbf{S} \mathbf{V}^T\|_F^2 \\ &= \|\mathbf{U}_{:,1:r} (\mathbf{S} \mathbf{V}^T)_{1:r,:}\|_F^2 \\ &= \|(\mathbf{S} \mathbf{V}^T)_{1:r,:}\|_F^2, \end{aligned} \quad (4)$$

where $\mathbf{0}$ is a zero matrix. Note that $\|\mathbf{W}\|_F^2 = \|\mathbf{S}\mathbf{V}^T\|_F^2$ and the square of Frobenius norm of a sub-matrix is usually smaller than the one of a whole matrix. Thus, the energy is likely to reduce after projection. Let \mathbf{x} denote the input data of a layer and $\hat{\mathbf{h}} = \mathbf{W}\mathbf{x}$. Then, the gradient $\frac{\partial \mathcal{L}}{\partial \mathbf{x}}$ is given by $\frac{\partial \mathcal{L}}{\partial \mathbf{x}} = \mathbf{W}^T \frac{\partial \mathcal{L}}{\partial \hat{\mathbf{h}}}$. After projection, the energy of the gradient becomes

$$\left\| \frac{\partial \mathcal{L}}{\partial \mathbf{x}} \right\|^2 = \|\mathcal{P}_{\Omega_r}(\mathbf{W})^T \mathbf{x}\|_F^2 = \|\mathbf{V}_{:,1:r} \mathbf{V}_{:,1:r}^T \mathbf{W}^T \frac{\partial \mathcal{L}}{\partial \hat{\mathbf{h}}}\|_F^2. \quad (5)$$

By similar deduction, we can conclude that the gradient energy $\|\frac{\partial \mathcal{L}}{\partial \mathbf{x}}\|$ is usually reduced after projection. We tend to face the problem of gradient vanishing as the network goes deeper.

To avoid gradient vanishing, we need to enlarge the gradient energy after projection. Note that SVD splits a system into a set of linearly independent components and the singular values represent the square root of the energy of the corresponding component [42]. The gradient energy reduction is due to the loss of weight matrix energy after projection. To get rid of gradient energy reduction, we propose to maintain the energy of the weight matrix with a simple solution that transfers the energy of the less important components to the more important ones instead of cutting them off. We use \mathbf{s} to denote the vector composed of the singular values of \mathbf{W} in descending order, i.e., $\mathbf{s} = \text{diag}(\mathbf{S})$, and use $\mathbf{s}_{1:r}$ to denote the first r elements of \mathbf{s} . To compensate for the reduced energy, we can update the first r singular values by multiplying them with a coefficient

$$\alpha = \|\mathbf{s}\| / \|\mathbf{s}_{1:r}\|. \quad (6)$$

Then, we replace the singular values in Eq. (2) with the updated ones, which can be equivalently represented by $\alpha \mathcal{P}_{\Omega_r}(\mathbf{W})$.

For the backward propagation, we have the following theorem for the expectation of gradient energy and gradient norm.

Theorem 1: \mathbf{W} and \mathbf{x} represent the learnable weight matrix and input data of a layer in the network, respectively. Let $\hat{\mathbf{h}} = \mathbf{W}\mathbf{x}$. Assume that $\mathbb{E}(\frac{\partial \mathcal{L}}{\partial \hat{\mathbf{h}}}) = \mathbf{0}$ and $\text{cov}(\frac{\partial \mathcal{L}}{\partial \hat{\mathbf{h}}}) = \sigma^2 \mathbf{I}$, where $\mathbf{0}$ is a zero matrix, \mathbf{I} is an identity matrix, and $\sigma > 0$ is a constant. We have $\mathbb{E}(\|\frac{\partial \mathcal{L}}{\partial \mathbf{x}}\|^2) = \sigma^2 \|\mathbf{W}\|_F^2$ and $\mathbb{E}(\|\frac{\partial \mathcal{L}}{\partial \mathbf{x}}\|) \leq \sigma \|\mathbf{W}\|_F$.

The proof of Theorem 1 is given in the appendix. Theorem 1 shows that the expectation of gradient energy and the upper bound of the expectation of gradient norm are kept if the Frobenius norm of \mathbf{W} is the same. Note that $\|\alpha \mathcal{P}_{\Omega_r}(\mathbf{W})\|_F = \|\mathbf{W}\|_F$. Our energy transfer strategy can keep the gradient energy and eases the trend of gradient vanishing.

C. BN Rectification

BN, which inserts a learnable layer to normalize each layer’s neuron activations as zero mean and unit variance, is popular in modern CNN. After training, the combination of a BN layer and its previous convolutional layer is equivalent to a new convolutional layer. This will affect the optimal low-rank approximation. Thus, when taking BN into account, we need to modify our energy transfer strategy. We have

$$\begin{aligned} \text{BN}(\mathbf{W}\mathbf{x}) &= \mathbf{\Gamma} \mathbf{\Sigma}^{-1} (\mathbf{W}\mathbf{x} - \boldsymbol{\mu}) + \boldsymbol{\beta} \\ &= \mathbf{\Gamma} \mathbf{\Sigma}^{-1} \mathbf{W}\mathbf{x} + (\boldsymbol{\beta} - \mathbf{\Gamma} \mathbf{\Sigma}^{-1} \boldsymbol{\mu}), \end{aligned} \quad (7)$$

where $\mathbf{\Gamma} \in \mathbb{R}^{N \times N}$ and $\mathbf{\Sigma} \in \mathbb{R}^{N \times N}$ are diagonal matrices containing trainable scalar parameters and the neuron-wise output standard deviation (a small constant is added for numerical stability), respectively, $\boldsymbol{\mu} \in \mathbb{R}^N$ is the mean output of the N neurons in the layer, and $\boldsymbol{\beta} \in \mathbb{R}^N$ is a trainable bias term. Taking $\tilde{\mathbf{W}} = \mathbf{\Gamma} \mathbf{\Sigma}^{-1} \mathbf{W}$ as a whole part, we can derive similar conclusion. Thus, when dealing with BN, we can rectify \mathbf{W} to $\tilde{\mathbf{W}}$ and apply our energy transfer strategy to $\tilde{\mathbf{W}}$. We denote the corresponding matrix of $\tilde{\mathbf{W}}$ after energy transfer as $\tilde{\mathbf{W}}'$. To figure out the estimation $\hat{\mathbf{W}}$ of the original weight matrix \mathbf{W} , we formulate it as the following optimization problem:

$$\min \|\mathbf{\Gamma} \mathbf{\Sigma}^{-1} \hat{\mathbf{W}} - \tilde{\mathbf{W}}'\|_F^2 \quad (8)$$

By letting the gradient be zero, we obtain the closed solution

$$\hat{\mathbf{W}} = [(\mathbf{\Gamma} \mathbf{\Sigma}^{-1})^T \mathbf{\Gamma} \mathbf{\Sigma}^{-1}]^{-1} (\mathbf{\Gamma} \mathbf{\Sigma}^{-1})^T \tilde{\mathbf{W}}'. \quad (9)$$

To avoid computing the inverse of singular matrix, we modify the solution to

$$\hat{\mathbf{W}} = [(\mathbf{\Gamma} \mathbf{\Sigma}^{-1})^T \mathbf{\Gamma} \mathbf{\Sigma}^{-1} + \epsilon]^{-1} (\mathbf{\Gamma} \mathbf{\Sigma}^{-1})^T \tilde{\mathbf{W}}', \quad (10)$$

where $\epsilon > 0$ is a small scalar and is set to 1e-5 in this paper. This process is called BN rectification. The proposed method is summarized in Algorithm 1.

D. Rank Setting

The ranks r_l ’s are hyperparameters and it is hard to set them layer by layer. We introduce a pruning ratio $p_l \in [0, 1]$ to determine the rank for the l^{th} layer. Mathematically, r_l is

Algorithm 1 Low-Rank Projection with Energy Transfer

Input:

The parameters $\Theta = \{\mathbf{W}^l, \mathbf{b}^l, \mathbf{\Gamma}^l, \beta^l | l = 1, 2, \dots, L\}$ of a network of L convolutional and BN layers, the neuron-wise output standard deviation matrices $\mathbf{\Sigma} \in \mathbb{R}^{N \times N}$ of the L BN layers, the desired ranks $\{r_l | l = 1, 2, \dots, L\}$ of the L layers, the total number of training iterations N , and a specified number T of iteration steps.

```

1: for  $n = 1, \dots, N$  do
2:   Update the parameters using SGD for one iteration.
3:   while training proceeds for every  $T$  iterations do
4:     for  $l = 1, \dots, L$  do
5:       Compute  $\widetilde{\mathbf{W}}^l = \mathbf{\Gamma}^l (\mathbf{\Sigma}^{-1})^l \mathbf{W}^l$ .
6:       Compute the SVD  $\widetilde{\mathbf{W}}^l \stackrel{\text{SVD}}{=} \mathbf{U}^l \mathbf{S}^l (\mathbf{V}^l)^T$ 
7:       Compute  $\alpha^l = \|\mathbf{s}^l\| / \|\mathbf{s}_{1:r_l}^l\|$  with  $\mathbf{s}^l = \text{diag}(\mathbf{S}^l)$ .
8:       Compute  $\hat{s}_i^l = \alpha^l s_i^l \forall 1, \dots, r_l$ .
9:       Update the first  $r_l$  diagonal entries of  $\mathbf{S}^l$  with
          $\{\hat{s}_i^l\}_1^{r_l}$  and set the remainders to zeros.
10:      Update  $\mathbf{W}^l$  with
          $[(\mathbf{\Gamma}^l (\mathbf{\Sigma}^l)^{-1})^T \mathbf{\Gamma}^l (\mathbf{\Sigma}^l)^{-1} + \epsilon]^{-1} (\mathbf{\Gamma}^l (\mathbf{\Sigma}^l)^{-1})^T \mathbf{U}^l \mathbf{S}^l (\mathbf{V}^l)^T$ .
11:     end for
12:   end while
13: end for

```

given by $(1-p_l) \min(N_l, N_{l-1})$. Then, the problem changes to how to set p_l 's. We find that manually setting p_l 's to the same value for all layers works well in practice. In the following, we use P to denote the unique rank pruning ratio.

The rank can be adaptively set through Bayesian optimization. It is a general framework for minimizing blackbox objective functions that are expensive to evaluate [43]. The goal is to trade off between network performance and model size. The objective function is given by

$$\min_{\mathbf{p}} \mathcal{E}(\mathbf{p}) + \lambda C(\mathbf{p}), \quad (11)$$

where $\mathbf{p} = [p_1, p_2, \dots, p_L]$, $\mathcal{E}(\mathbf{p})$ is the top-1 error of the compressed model, $C(\mathbf{p})$ is the compression rate, and λ is the trade-off parameter. $C(\mathbf{p})$ is defined by $C(\mathbf{p}) = D(\mathbf{p})/D_{\text{ori}}$, where $D(\mathbf{p})$ and D_{ori} are respectively the sizes of the compressed and the original models. We model the objective function as a Gaussian process and use the expected improvement for evaluation to select the most promising candidate. We refer readers to the work [44] for more details. To save searching time, the top-1 error $\mathcal{E}(\mathbf{p})$ can be estimated by training with much fewer epochs than ordinary training.

Note that the Bayesian optimization is not part of LRPET. We just show that our method is compatible to hyper parameters (rank ratios) search. We should emphasize that our method works well with a unique rank ratio without searching. Without confusion, we will use LRPET-S to denote LRPET with Bayesian optimization for searching.

E. Network Inference

After training by LRPET, the singular values outside the range $[1, r_l]$ are near zero at each layer. We can set these small singular values to zeros without performance degeneration. For

inference, an ordinary convolutional layer changes into two cascaded small layers. Given the skinny SVD $\mathbf{W} = \mathbf{U}\mathbf{S}\mathbf{V}^T$, we construct the weight matrices of the two layers with $\mathbf{U}\sqrt{\mathbf{S}}$ and $\sqrt{\mathbf{S}}\mathbf{V}^T$. Suppose $\mathbf{W} \in \mathbb{R}^{m \times n}$ and the rank is r . The number of parameters changes from mn to $(m+n)r$, and the computational complexity of $\mathbf{W}\mathbf{x}$ also changes from $O(mn)$ to $O((m+n)r)$. If r is small enough, such factorization will greatly reduce parameters and computational cost.

IV. EXPERIMENTS

In this section, LRPET is evaluated on two benchmark image classification datasets CIFAR-10 [24] and ImageNet [2]. Several mainstream CNN models are taken into account, including ResNets [1], VGG-16 [22] and GoogLeNet [23]. Note that VGG-16 is a modified version of the original following [36]. Our experiments are implemented with PyTorch [45].

A. Datasets and Experimental Setting

1) *Datasets*: The CIFAR-10 dataset contains 60,000 color images with the size of 32×32 . The images in the CIFAR-10 dataset are divided into 10 classes and each class has 5,000 training images and 1,000 testing images. We train the network according to standard data enhancement [46], [47]. For training, each image side is first zero-padded with 4 pixels, and then a 32×32 patch is randomly cropped from the padded image or its horizontal flip with a probability of 0.5. We directly use the original 32×32 images for test. There are 1.28 million training images and 50,000 validation images of 1,000 classes in ImageNet dataset [2]. Default ImageNet setting of PyTorch for data augmentation is adopted.

2) *Experimental Setting*: Training is based on SGD with a batch size of 128, a momentum of 0.9, and a weight decay of $5e-4$. The initial learning rate is set to 0.1 and is divided by ten at the 50% and 75% of the total epoch number. We train the networks from scratch with LRPET for 400 epochs. The results of baselines of quoted from CC [48]. On ImageNet, networks are trained from scratch with LRPET for 120 epochs with batch size of 256 and initial learning rate of 0.1. The learning rate is divided by 10 at epochs 30, 60, and 90.

Note that a lot of compared methods use pre-trained model. For fair comparison, we also conduct experiments that first use the pre-trained models as initialization and then apply LRPET. On CIFAR-10, the pre-trained model is taken from CC [48] or trained by ourselves with SGD for 164 epochs. The other training settings are the same as above. The pre-trained models on ImageNet are taken from PyTorch. When applying LRPET, the training epoch numbers for CIFAR-10 and ImageNet are 200 and 120, respectively. The other training settings are the same as training from scratch except that the initial learning rate is set to 0.01. In the following experimental results, we will use ‘‘Y’’ and ‘‘N’’ in a ‘‘PT?’’ column to indicate whether using pre-trained model or not, respectively.

We set the iteration interval T to one epoch on CIFAR-10 and 500 iterations for ImageNet. All the experiments of LRPET on CIFAR-10 are repeated for three times. For rank ratio searching, the iteration number of Bayesian optimization is set to 20 and the trade-off parameter λ is set to 1. When

TABLE I: Results of ResNet-56 on CIFAR-10

Method	PT?	Acc. (%)	FLOPs (PR)	Params (PR)
Baseline	N	93.33	125.49M (0.0%)	0.85M (0.0%)
NISP [31]	N	93.01	81.00M (35.5%)	0.49M (42.4%)
GAL-0.6 [38]	N	92.98	78.30M (37.6%)	0.75M (11.8%)
DECORE-200 [39]	Y	93.26	62.93M (49.9%)	0.43M (49.0%)
HRank [36]	Y	93.17	62.72M (50.0%)	0.49M (42.4%)
LRPET ($P=0.55$)	N	93.07±0.33	61.20M (51.2%)	0.41M (51.8%)
LRPET ($P=0.55$)	Y	93.43±0.16	61.20M (51.2%)	0.41M (51.8%)
LRPET* ($P=0.55$)	Y	93.68±0.17	61.20M (51.2%)	0.41M (51.8%)
CC† ($C=0.5$) [48]	Y	93.53±0.11	60.99M (51.4%)	0.45M (47.0%)
CC ($C=0.5$) [48]	Y	93.64	60.00M (52.0%)	0.44M (48.2%)
SFP [30]	N	92.26±0.31	59.48M (52.6%)	-
FTWT _J ($r=0.88$) [40]	Y	92.28	57.73M (54.0%)	-
LRPET ($P=0.57$)	N	92.99±0.21	56.06M (55.3%)	0.39M (53.5%)
GAL-0.8 [38]	N	90.36	49.99M (60.2%)	0.29M (65.9%)
FTWT _D ($r=0.80$)	Y	92.63	42.66M (66.0%)	-
LRPET ($P=0.70$)	N	92.13±0.17	38.57M (69.2%)	0.27M (67.4%)
LRPET ($P=0.70$)	Y	92.71±0.14	38.57M (69.2%)	0.27M (67.4%)
HRank [36]	N	90.72	32.52M (74.1%)	0.27M (68.2%)
LRPET ($P=0.80$)	N	91.13±0.59	26.23M (79.1%)	0.17M (79.0%)
LRPET-S	N	91.24±0.23	24.13M (80.8%)	0.18M (78.9%)

TABLE II: Results of ResNet-110 on CIFAR-10

Method	PT?	Acc. (%)	FLOPs (PR)	Params (PR)
Baseline	N	93.50	252.89M(0.0%)	1.72M(0.0%)
SFP [30]	N	93.38±0.30	149.71M (40.8%)	-
GAL-0.5 [38]	N	92.55	130.20M (48.5%)	0.95M (44.8%)
HRank [36]	N	93.36	105.70M (58.2%)	0.70M (59.3%)
LFPC [37]	N	93.07	100.40M (60.3%)	-
DECORE-300 [39]	Y	93.50	96.66M (61.8%)	0.61M (64.8%)
LRPET ($P=0.65$)	N	93.61±0.19	93.78M (62.9%)	0.65M (61.8%)

evaluating the classification error for Bayesian optimization, each model is trained with 60 epochs and the learning rate is divided by 10 for every 20 epochs. Specifically, since searching for ImageNet is too time consuming, we search the hyperparameters on CIFAR-10 and then apply it to ImageNet.

B. Image Classification Results

1) *Results on CIFAR-10*: We compare LRPET with other low-rank compression and network pruning methods by conducting experiments on CIFAR-10 with ResNets, VGG-16, and GoogLeNet.

ResNets. We report the classification accuracy, FLOPs, and parameter sizes accompanied with the corresponding pruning rate (PR) of ResNet-56 and ResNet-110 in Tables I and II, respectively. We change the rank pruning ratio P of LRPET to get results with different FLOPs and parameter sizes. The dashed lines separate results with the same order of FLOPs and the best results are marked in bold. Note that the data augmentation used by CC [48] is not the same as the standard one, i.e., each image side is zero-padded with 8 pixels. For fair comparison, we also use the same configuration as CC [48] for training, denoted by LRPET*. Since CC [48] only provides the result of one trial, for more thorough comparison, we also reproduce their experiment with the official provided code for three times, denoted by CC†.

We can see that, compared with other methods, LRPET achieves higher accuracy with less or comparable FLOPs and

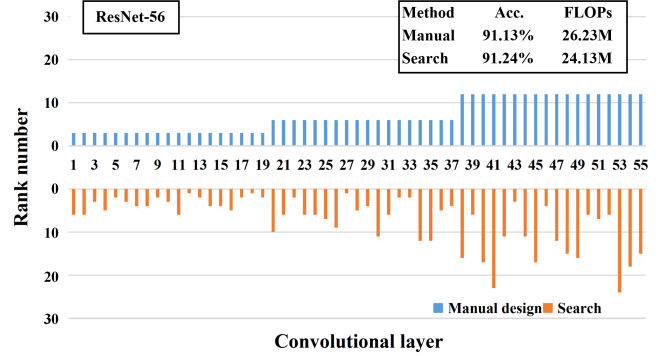


Fig. 2: Layer rank comparison

parameters for both size of ResNets. Note that our result is more convincing since we report the average result of three trials while most compared methods only report the result of one trial. Compare with the compared state-of-the-art pruning methods, the success of LRPET reveals that the overlooked low-rankness can outperform pruning method with proper design. Note that FTWT is a dynamic pruning method, which is expected to outperform static compression method the pruned network structure adaptively changes according to different samples. However, LRPET still outperforms it at different computation budgets. The results of ResNet-110 show that LRPET without pre-training even outperforms the pruning method DECORE with pre-trained model. Although LRPET with default data augmentation performs a little poorer than CC, LRPET outperforms CC when using the same data augmentation, and the superiority is more significant in the case of multiple trials. It is worth noting that CC is the combination of low-rank decomposition and pruning while LRPET only utilizes low-rankness. Besides, LRPET trains the network only for 200 epochs, but CC needs 300 epochs.

We conduct Bayesian optimization experiment on ResNet-56 to show that our result can be further improved by searching hyperparameters. From Table I, LRPET-S achieves higher reduction of FLOPs (80.8% vs. 79.1%) with better performance (91.24% vs. 91.13%) than LRPET. We also display the rank number of different layers for the two methods in Fig. 2. We can see that LRPET-S adaptively set the rank pruning ratio for different layers, which suggests that different layers has different sensitivity to network compression.

Note that for the shortcut between residual blocks with different channel numbers, TRP [20] and SVD training [21] use 1×1 convolution (shortcut B) while the other methods adopt the padding strategy (shortcut A). To compare with them, following TRP, we apply LRPET to ResNet 20/56 with shortcut B (denoted by ResNet-20/56-B) for 164 epochs. To show that our superiority does not simply come from weight decay setting, we re-implement TRP for the weight decay of $5e-4$ and quote the result for the weight decay of $1e-4$ from their paper. Following the official code of TRP, we also fine-tune the networks for four epochs in our re-implementation. Since the speeding up of TRP varies in different trials, we report the one with the best accuracy from three trials for TRP re-implementation. Note that SVD training utilize pre-training

TABLE III: Results of ResNet-20/56-B on CIFAR-10

Method	Acc. (%)	Speed up
ResNet-20-B (Baseline, wd=1e-4)	91.74	1.00×
ResNet-20-B (Baseline, wd=5e-4)	92.40	1.00×
ResNet-20-B (TRP1, wd=1e-4)	90.12	1.97×
ResNet-20-B (TRP1+Nu, wd=1e-4)	90.50	2.17×
ResNet-20-B (TRP1, wd=5e-4)	86.00	1.30×
ResNet-20-B (TRP1+Nu, wd=5e-4)	85.52	1.27×
ResNet-20-B (LRPET, wd=5e-4, $P=0.60$)	90.62±0.24	2.34×
ResNet-20-B (SVD training [21], wd=1e-4)	90.97	2.20×
ResNet-20-B (LRPET#, wd=5e-4, $P=0.60$)	91.56±0.10	2.34×
ResNet-56-B (Baseline, wd=1e-4)	93.14	1.00×
ResNet-56-B (Baseline, wd=5e-4)	93.52	1.00×
ResNet-56-B (TRP, wd=1e-4)	92.77	2.31×
ResNet-56-B (TRP, wd=5e-4)	92.72	1.57×
ResNet-56-B (TRP+Nu, wd=5e-4)	92.16	1.50×
ResNet-56-B (LRPET, wd=5e-4, $P=0.65$)	92.89±0.08	2.50×
ResNet-56-B (SVD training [21], wd=1e-4)	93.67	2.70×
ResNet-56-B (LRPET#, wd=5e-4, $P=0.69$)	93.69±0.18	3.01×
ResNet-56-B (TRP1+Nu, wd=1e-4)	91.85	4.48×
ResNet-56-B (LRPET, wd=5e-4, $P=0.81$)	92.05±0.19	4.44×

and fine-tuning, which results in three times of total training epochs. For fair comparison, we also conduct experiment of LRPET with pre-trained models, denoted by LRPET#. The settings are the same as the above experiments except that the training epoch number of LRPET is 300. The results are shown in Table III. The performance gain of LRPET over optimal result of TRP is significant. We should emphasize that TRP needs to use SVD for every iteration to guarantee good performance, which spends much more time than LRPET. Besides, the four epochs of fine-tuning effectively improve TRP’s performance while LRPET does not need fine-tuning to achieve the good performance. SVD training is better than LRPET trained with 164 epochs, but the superiority comes from more training epochs. When training with fair number of epochs, LRPET outperforms SVD training, which shows that preserving the model capacity improves the performance.

GoogLeNet. The results of GoogLeNet on CIFAR-10 are shown in Table IV. LRPET achieves the highest accuracy with the smallest FLOPs. It even outperforms baseline when cutting about half of the FLOPs and parameters. Without pre-training, LRPET outperforms pruning methods with pre-trained models (DECORE, CC, and HRank). This again demonstrates the potential of low-rankness for network compression. Compare with the pruning method GAL that also trains from scratch, the performance gain of LRPET is significant (more than 1%).

TABLE IV: Results of GoogLeNet on CIFAR-10

Method	PT?	Acc. (%)	FLOPs (PR)	Params (PR)
Baseline	N	95.05	1.52B(0.0%)	6.15M(0.0%)
DECORE-500 [39]	Y	95.20	1.22B (19.8%)	4.73M (23.0%)
GAL-0.05 [38]	N	93.93	0.94B (38.2%)	3.12M (49.3%)
CC ($C=0.5$) [48]	Y	95.18	0.76B (50.0%)	2.83M (54.0%)
LRPET ($P=0.60$)	N	95.25±0.23	0.74B (51.4%)	3.03M (50.8%)
HRank [36]	Y	94.53	0.69B(54.6%)	2.74M (55.4%)
CC ($C=0.6$) [48]	Y	94.88	0.61B (59.9%)	2.26M (63.3%)
LRPET ($P=0.68$)	N	94.97±0.10	0.59B (61.3%)	2.41M (60.8%)

VGG-16. Since the channel number of each layer of VGG-16 varies significantly, to avoid too few channels, we set the smallest ranks of the first two layers to 2/3 of the original

matrix ranks and the minimum ranks of the other convolutional layers to the minimum rank of the second convolutional layer. Table V displays the results of VGG-16 on CIFAR-10. Although LRPET without pre-training is a little poorer than methods with pre-trained models for some computation budgets, the performance of LRPET is significantly improved when using pre-trained model for initialization and finally outperforms the other pre-trained methods. Using pre-trained model in practice usually means nearly twice of total training time. We should emphasize that pre-trained model is necessary for these compared methods but is optional for LRPET. Without pre-training, LRPET still works well and is significantly better than the training from scratch method GAL.

TABLE V: Results of VGG-16 on CIFAR-10

Method	PT?	Acc. (%)	FLOPs (PR)	Params (PR)
Baseline	N	93.70	313.2M (0.0%)	14.72M (0.0%)
GAL-0.05 [38]	N	92.03	189.49M (39.6%)	3.36M (77.6%)
GAL-0.1 [38]	N	90.73	171.89M (45.2%)	2.67M (82.2%)
HRank [36]	Y	93.43	145.61M (53.5%)	2.51M (82.9%)
LRPET ($P=0.63$)	N	93.49±0.14	144.10M (54.0%)	6.12M (58.5%)
LRPET ($P=0.63$)	Y	93.86±0.25	144.10M (54.0%)	6.12M (58.5%)
FTWT _D ($r=0.92$) [40]	Y	93.73	137.81M (56.0%)	-
LRPET ($P=0.65$)	N	93.46±0.10	137.78M (56.0%)	5.79M (60.6%)
LRPET ($P=0.65$)	Y	93.76±0.12	137.78M (56.0%)	5.79M (60.6%)
DECORE-200 [39]	Y	93.56	110.51M (64.8%)	1.66M (89.0%)
FTWT _J ($r=0.92$) [40]	Y	93.55	109.62M (65.0%)	-
HRank [36]	Y	92.34	108.61M (65.3%)	2.64M (82.4%)
LRPET ($P=0.77$)	N	93.27±0.17	107.56M (65.7%)	3.83M (74.0%)
LRPET ($P=0.77$)	Y	93.70±0.14	107.56M (65.7%)	3.83M (74.0%)
FTWT _D ($r=0.85$) [40]	Y	93.19	84.56M (73.0%)	-
FTWT _J ($r=0.88$) [40]	Y	92.65	81.43M (74.0%)	-
LRPET ($P=0.92$)	N	92.93±0.11	81.29M (74.1%)	1.62M (88.9%)
LRPET ($P=0.92$)	Y	93.52±0.05	81.29M (74.1%)	1.62M (88.9%)

2) *Results on ImageNet:* To show the generalization ability of LRPET, experiments on large-scale dataset ImageNet with ResNet 18/34/50 are conducted and the results are shown in Table VI. We can see that LRPET also outperforms the other state-of-the-art low-rank decomposition and pruning methods. It achieves the highest top-1 and top-5 accuracy with the smallest FLOPs for all the three networks. At most FLOPs orders, LRPET without pre-training performs better than methods either with or without pre-training. When pre-trained models are utilized, the top-1 accuracy of LRPET is improved with more than 1% and achieves the best performance for all the cases. Specifically, compared with baseline, LRPET for ResNet-50 shows only 0.24% decrease in top-1 accuracy when the FLOPs reduction rate is 53.6%. From the results of ResNet-50, we empirically find that the superiority of LRPET is more prominent for larger FLOPs reduction rate. When $P=0.80$, the performance gain of LRPET without pre-training over the second best method (pre-trained pruning method DECORE) is 1.26%, which is very significant for large-scale dataset. Compare with the baseline of ResNet-18, LRPET ($P=0.80$) achieves higher accuracy with only near half of the FLOPs. For the hyper-parameter search experiment of LRPET-S, although rank pruning ratios are searched on CIFAR-10, they are transferable to ImageNet. LRPET-S with and without pre-training achieve higher accuracy with smaller FLOPs than all the compared methods of the same FLOPs order.

TABLE VI: Results of ResNets on ImageNet

Model	Method	PT?	Top-1 Acc. (%)	Top-5 Acc. (%)	FLOPs (PR)	Params (PR)
ResNet-18	Baseline	N	69.76	89.08	1.82B (0.0%)	11.69M (0.0%)
	SFP [30]	N	67.10	87.78	1.06B (41.8%)	-
	TRP [20]	N	65.46	86.48	1.01B (44.5%)	-
	FTWT ($r=0.91$) [40]	Y	67.49	-	0.88B (51.6%)	-
	LRPET ($P=0.58$)	N	67.87	88.04	0.86B (52.5%)	5.81M (50.2%)
ResNet-34	Baseline	N	73.31	91.42	3.66B (0.0%)	21.78M (0.0%)
	SFP [30]	N	71.83	90.33	2.16B (41.1%)	-
	FTWT ($r=0.92$) [40]	Y	71.71	-	1.75B (52.2%)	-
	LRPET ($P=0.58$)	N	71.84	90.48	1.71B (53.1%)	10.51M (51.7%)
	LRPET ($P=0.58$)	Y	72.95	90.98	1.71B (53.1%)	10.51M (51.7%)
ResNet-50	Baseline	N	76.15	92.87	4.09B (0.0%)	25.50M (0.0%)
	SFP [30]	N	74.61	92.06	2.38B (41.8%)	-
	DECORE-6 [39]	Y	74.58	92.18	2.36B (42.3%)	14.10M (44.71%)
	GAL-0.5 [38]	N	71.95	90.94	2.33B (43.0%)	21.20M (16.9%)
	HRank [36]	Y	74.98	92.33	2.30B (43.9%)	16.15M (36.7%)
	TRP+Nu [20]	N	74.06	92.07	2.27B (44.5%)	-
	CC ($C=0.5$) [48]	Y	75.59	92.64	1.93B (52.9%)	13.2M (48.4%)
	LRPET ($P=0.62$)	N	74.25	91.93	1.90B (53.6%)	12.89M (49.5%)
	LRPET ($P=0.62$)	Y	75.91	92.79	1.90B (53.6%)	12.89M (49.5%)
	GAL-0.5-joint [38]	N	71.80	90.92	1.84B (55.0%)	19.31M (24.3%)
	DECORE-5 [39]	Y	72.06	90.82	1.60B (60.9%)	8.87M (65.2%)
	HRank [36]	N	71.89	91.01	1.55B (62.1%)	13.77M (46.0%)
	LRPET-S	N	72.50	90.99	1.38B (66.2%)	9.18M (64.0%)
	LRPET-S	Y	73.72	91.73	1.38B (66.2%)	9.18M (64.0%)
	DECORE-4 [39]	Y	69.71	89.37	1.19B (70.9%)	6.12M (76.0%)
	GAL-1-joint [38]	N	69.31	89.12	1.11B (72.9%)	10.12M (60.3%)
HRank [36]	N	69.10	89.58	0.98B (76.0%)	8.27M (67.6%)	
LRPET ($P=0.80$)	N	70.97	90.16	0.98B (76.0%)	7.74M (70.0%)	

C. Ablation Study

Here we conduct ablation studies to investigate the contributions of each component in our proposed LRPET. ResNet-56 and VGG-16 on CIFAR-10 are taken into account. We train the networks from scratch. The pruning rate P is set to 0.57 and 0.92 for ResNet-56 and VGG-16, respectively.

1) *Energy Transfer and BN Rectification*: We study the effects of energy transfer and BN rectification by removing them. The experiment results are shown in Table VII. Here “Low-Rank Projection” denotes applying LRP at the end of each epoch without energy transfer or BN rectification. When using energy transfer without BN rectification, the results are better than Low-Rank Projection. This verifies that energy transfer can ease the gradient energy reduction problem in Low-Rank Projection. Using BN rectification without energy transfer also improves the results of Low-Rank Projection, which suggests that the incompatibility between BN and convolution for LRP is well solved by BN rectification. LRPET that adopts both strategies can further improve the performance. This shows that energy transfer and BN rectification have a collaborative effect for the final performance.

TABLE VII: Accuracy (%) comparison on CIFAR-10 for energy transfer and BN rectification

Method	ResNet-56	VGG-16
Low-Rank Projection	92.68	92.77
LRPET (w/o BN Rectification)	92.94	92.82
LRPET (w/o Energy Transfer)	92.83	92.80
LRPET	92.99	92.93

2) *Training Strategy*: To show the superiority of our training strategy, we compare LRPET with three intuitive training

strategies. The first one “From Scratch” is to decompose a random initialized network into low-rank form and train it from scratch. The second one “Fine Tuning” is directly decomposing a pre-trained baseline model and fine-tuning it. Here we fine-tune the network for 40 epochs with a learning rate of 0.001. The third one “Early Stop & Ordinary Training” refers to training the model with LRPET, stopping at the 200th epoch, and then continuing training the decomposed network to 400 epochs with the same learning rate as ordinary training. This strategy aims to investigate whether LRPET only provides a good initialization or works for the whole training process.

The results are shown in Table VIII. Training low-rank decomposition network from scratch performs the worst. This is because low-rank decomposition means lower model capacity and leads to a much deeper network, which makes optimization more difficult. Fine-tuning the fully trained model significantly improves the performance. However, it is still much worse than LRPET. This suggests that a well-trained model in Euclidean space does not provide a good initialization for optimization in the low-rank manifold. An early stop of LRPET provides a initialization for low-rank network but is not good enough. This is because the model does not close to the low-rank manifold enough at the stopped epoch. Thus, applying LRPET for the whole training process is needed.

3) *Amplification coefficient α* : We transfer energy with an adaptive amplification coefficient α to keep the energy. In order to verify the effectiveness of such a strategy, we compared the performance of the network using different fixed values of α and our adaptive strategy. Fig. 3 illustrates the test accuracy curves of different α settings for ResNet-56 and

TABLE VIII: Accuracy (%) comparison on CIFAR-10 with different training strategies

Method	ResNet-56	VGG-16
From Scratch	62.62	57.59
Fine Tuning	90.83	90.37
Early Stop & Ordinary Training	90.61	91.41
LRPET	92.99	92.93

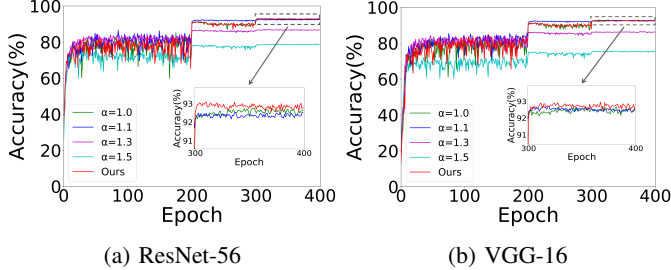


Fig. 3: Test accuracy curves of different α

VGG-16 on CIFAR-10. When α is small, the accuracy can be improved, which shows that the reduction of gradient energy will degrade the performance and can be recovered by energy compensation. When α is too large, the weight will deviate from the optimal solution and the result is poorer than without energy compensation. In contrast, the adaptive amplification coefficient α has better performance than all fixed values of α , which demonstrates that keeping the energy of weight matrix the same is effective for training low-rank networks.

D. Training Time Consumption

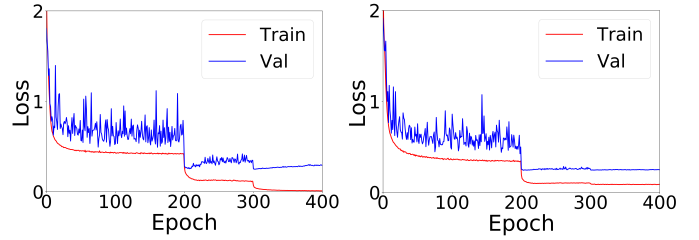
Although the computation complexity of SVD is high, SVD is only used at the end of each epoch or a certain number of iterations in LRPET and the training time increment is small. TRP [20] also utilizes SVD for training, but it is very time-consuming since it needs SVD for every iteration. In Table IX, we show the average training time of one epoch of LRPET and TRP for ResNet-56, ResNet-110, and VGG-16 on CIFAR-10 for comparison. Compared to the original SGD, the relative additional training time of LRPET is small, while TRP takes multiple times of training time of LRPET. When nuclear norm regularization is included, the training time of TRP will further increase. For example, training ResNet-56 on CIFAR-10, the relative additional training time of LRPET compared to original SGD is only +3.2%, while TRP is +371%, which verifies that our LRPET is a simple and efficient method.

TABLE IX: Training time (seconds) on CIFAR-10

Method	ResNet-56	ResNet-110	VGG-16
Baseline	25.0	48.2	17.2
LRPET	25.8 (+3.2%)	48.6 (+0.8%)	18.8 (+9.3%)
TRP [20]	117.8 (+371%)	229.3 (+376%)	171.8 (+899%)
TRP+Nu [20]	139.2 (+457%)	241.2 (+400%)	175.8 (+922%)

E. Convergence Analysis

Our optimization method is a variant of projected SGD (PSGD). The theoretical convergence analysis of PSGD has



(a) ResNet-56 (b) VGG-16

Fig. 4: Training and test loss curves

only been given for convex problems but the optimization of a deep neural network is highly nonconvex. Even for the simple SGD on a deep neural network, its convergence property is not thoroughly studied. However, PSGD works well in practice. In Fig. 4, we plot the LRPET’s loss curves of training and test for ResNet-56 and VGG-16 on CIFAR-10. We can see that, LRPET converges well in practice. In most experiments, the relative errors between the original matrix and the product of the decomposed matrices for all the layers are smaller than 2% and the accuracy of the decomposed network also maintains almost the same as the original network, which suggests that the optimized matrices are numerical low-rank.

V. CONCLUSION

Low-rankness is a popular property for compression in traditional learning, but it is not so popular in compressing deep neural networks. This is because a neural network with low-rank constraint is hard to train. Compared to other network compression methods, low-rank-based methods seem less competitive. In this paper, we propose a new training method that efficiently trains low-rank constraint network with considerable good results. We reveal that the potential effectiveness of low-rankness is neglected in network compression. LRPET not only outperforms the other low-rank compression method but also some state-of-the-art pruning methods.

REFERENCES

- [1] K. He, X. Zhang, S. Ren, and J. Sun, “Deep residual learning for image recognition,” in *Proceedings of the IEEE Conference on Computer Vision and Pattern Recognition*, 2016, pp. 770–778.
- [2] O. Russakovsky, J. Deng, H. Su, J. Krause, S. Satheesh, S. Ma, Z. Huang, A. Karpathy, A. Khosla, M. S. Bernstein, A. C. Berg, and L. Fei-Fei, “Imagenet large scale visual recognition challenge,” *International Journal of Computer Vision*, vol. 115, no. 3, pp. 211–252, 2015.
- [3] S. Ren, K. He, R. B. Girshick, and J. Sun, “Faster R-CNN: towards real-time object detection with region proposal networks,” *IEEE Transactions on Pattern Analysis and Machine Intelligence*, vol. 39, no. 6, pp. 1137–1149, 2017.
- [4] W. Wen, C. Xu, C. Wu, Y. Wang, Y. Chen, and H. Li, “Coordinating filters for faster deep neural networks,” in *Proceedings of the IEEE Conference on Computer Vision and Pattern Recognition*, 2017, pp. 658–666.
- [5] X. Yu, T. Liu, X. Wang, and D. Tao, “On compressing deep models by low rank and sparse decomposition,” in *Proceedings of the IEEE Conference on Computer Vision and Pattern Recognition*, July 2017, pp. 7370–7379.
- [6] X. Zhang, J. Zou, K. He, and J. Sun, “Accelerating very deep convolutional networks for classification and detection,” *IEEE Transactions on Pattern Analysis and Machine Intelligence*, vol. 38, no. 10, pp. 1943–1955, 2015.

- [7] H. Kim, M. U. K. Khan, and C. Kyung, "Efficient neural network compression," in *Proceedings of the IEEE Conference on Computer Vision and Pattern Recognition*, 2019, pp. 12 569–12 577.
- [8] F. Tung and G. Mori, "CLIP-Q: deep network compression learning by in-parallel pruning-quantization," in *Proceedings of the IEEE Conference on Computer Vision and Pattern Recognition*, 2018, pp. 7873–7882.
- [9] M. Lin, R. Ji, Y. Zhang, B. Zhang, Y. Wu, and Y. Tian, "Channel pruning via automatic structure search," in *Proceedings of the International Joint Conference on Artificial Intelligence*, 2020, pp. 673–679.
- [10] D. Li, S. Chen, X. Liu, Y. Sun, and L. Zhang, "Towards optimal filter pruning with balanced performance and pruning speed," in *Proceedings of the Asian Conference on Computer Vision*, vol. 12625, 2020, pp. 252–267.
- [11] J. Wu, C. Leng, Y. Wang, Q. Hu, and J. Cheng, "Quantized convolutional neural networks for mobile devices," in *Proceedings of the IEEE Conference on Computer Vision and Pattern Recognition*, 2016, pp. 4820–4828.
- [12] G. Hinton, O. Vinyals, J. Dean *et al.*, "Distilling the knowledge in a neural network," *arXiv preprint arXiv:1503.02531*, vol. 2, no. 7, 2015.
- [13] K. Guo, L. Liu, X. Xu, D. Xu, and D. Tao, "Godex+: Fast and robust low-rank matrix decomposition based on maximum correntropy," *IEEE Transactions on Neural Networks and Learning Systems*, vol. 29, no. 6, pp. 2323–2336, 2018.
- [14] G. Liu, Z. Lin, S. Yan, J. Sun, Y. Yu, and Y. Ma, "Robust Recovery of Subspace Structures by Low-Rank Representation," *IEEE Transactions on Pattern Analysis and Machine Intelligence*, vol. 35, no. 1, pp. 171–184, Jan. 2013.
- [15] R. He, B.-G. Hu, W.-S. Zheng, and X.-W. Kong, "Robust Principal Component Analysis Based on Maximum Correntropy Criterion," *IEEE Trans. Image Process.*, vol. 20, no. 6, pp. 1485–1494, Jun. 2011.
- [16] J. Wright, A. Y. Yang, A. Ganesh, S. S. Sastry, and Y. Ma, "Robust Face Recognition via Sparse Representation," *IEEE Transactions on Pattern Analysis and Machine Intelligence*, vol. 31, no. 2, pp. 210–227, Feb. 2009.
- [17] E. Elhamifar and R. Vidal, "Sparse Subspace Clustering: Algorithm, Theory, and Applications," *IEEE Transactions on Pattern Analysis and Machine Intelligence*, vol. 35, no. 11, pp. 2765–2781, Nov. 2013.
- [18] M. Yang, L. Zhang, J. Yang, and D. Zhang, "Robust Sparse Coding for Face Recognition," in *Proceedings of the IEEE Conference on Computer Vision and Pattern Recognition*, Jun. 2011, pp. 625–632.
- [19] M. Jaderberg, A. Vedaldi, and A. Zisserman, "Speeding up convolutional neural networks with low rank expansions," in *Proceedings of the British Machine Vision Conference*, 2014.
- [20] Y. Xu, Y. Li, S. Zhang, W. Wen, B. Wang, Y. Qi, Y. Chen, W. Lin, and H. Xiong, "TRP: trained rank pruning for efficient deep neural networks," in *Proceedings of the International Joint Conference on Artificial Intelligence*, 2020, pp. 977–983.
- [21] H. Yang, M. Tang, W. Wen, F. Yan, D. Hu, A. Li, H. Li, and Y. Chen, "Learning low-rank deep neural networks via singular vector orthogonality regularization and singular value sparsification," in *Proceedings of the IEEE Conference on Computer Vision and Pattern Recognition, Workshops*, 2020, pp. 2899–2908.
- [22] K. Simonyan and A. Zisserman, "Very deep convolutional networks for large-scale image recognition," in *Proceedings of the International Conference on Learning Representations*, 2015.
- [23] C. Szegedy, W. Liu, Y. Jia, P. Sermanet, S. E. Reed, D. Anguelov, D. Erhan, V. Vanhoucke, and A. Rabinovich, "Going deeper with convolutions," in *Proceedings of the IEEE Conference on Computer Vision and Pattern Recognition*, 2015, pp. 1–9.
- [24] A. Krizhevsky and G. Hinton, "Learning multiple layers of features from tiny images," *Technical report, University of Toronto*, 2009.
- [25] V. Lebedev, Y. Ganin, M. Rakhuba, I. V. Oseledets, and V. S. Lempitsky, "Speeding-up convolutional neural networks using fine-tuned cp-decomposition," in *Proceedings of the International Conference on Learning Representations*, 2015.
- [26] S. Lin, R. Ji, C. Chen, D. Tao, and J. Luo, "Holistic CNN compression via low-rank decomposition with knowledge transfer," *IEEE Transactions on Pattern Analysis and Machine Intelligence*, vol. 41, no. 12, pp. 2889–2905, 2019.
- [27] Y. Li, S. Gu, C. Mayer, L. V. Gool, and R. Timofte, "Group sparsity: The hinge between filter pruning and decomposition for network compression," in *Proceedings of the IEEE Conference on Computer Vision and Pattern Recognition*, 2020, pp. 8015–8024.
- [28] J. M. Alvarez and M. Salzmann, "Compression-aware training of deep networks," in *Proceedings of the Advances in Neural Information Processing Systems*, 2017, pp. 856–867.
- [29] S. Han, H. Mao, and W. J. Dally, "Deep compression: Compressing deep neural network with pruning, trained quantization and Huffman coding," in *Proceedings of the International Conference on Learning Representations*, 2016.
- [30] Y. He, G. Kang, X. Dong, Y. Fu, and Y. Yang, "Soft filter pruning for accelerating deep convolutional neural networks," in *Proceedings of the International Joint Conference on Artificial Intelligence*, 2018, pp. 2234–2240.
- [31] R. Yu, A. Li, C. Chen, J. Lai, V. I. Morariu, X. Han, M. Gao, C. Lin, and L. S. Davis, "NISP: pruning networks using neuron importance score propagation," in *Proceedings of the IEEE Conference on Computer Vision and Pattern Recognition*, 2018, pp. 9194–9203.
- [32] H. Li, A. Kadav, I. Durdanovic, H. Samet, and H. P. Graf, "Pruning filters for efficient convnets," in *Proceedings of the International Conference on Learning Representations*, 2017.
- [33] Y. He, X. Zhang, and J. Sun, "Channel pruning for accelerating very deep neural networks," in *Proceedings of the IEEE International Conference on Computer Vision*, 2017, pp. 1398–1406.
- [34] J. Luo, H. Zhang, H. Zhou, C. Xie, J. Wu, and W. Lin, "ThiNet: Pruning CNN filters for a thinner net," *IEEE Transactions on Pattern Analysis and Machine Intelligence*, vol. 41, no. 10, pp. 2525–2538, 2019.
- [35] Z. Liu, J. Li, Z. Shen, G. Huang, S. Yan, and C. Zhang, "Learning efficient convolutional networks through network slimming," in *Proceedings of the IEEE International Conference on Computer Vision*, 2017, pp. 2755–2763.
- [36] M. Lin, R. Ji, Y. Wang, Y. Zhang, B. Zhang, Y. Tian, and L. Shao, "Hrank: Filter pruning using high-rank feature map," in *Proceedings of the IEEE Conference on Computer Vision and Pattern Recognition*, 2020, pp. 1526–1535.
- [37] Y. He, Y. Ding, P. Liu, L. Zhu, H. Zhang, and Y. Yang, "Learning filter pruning criteria for deep convolutional neural networks acceleration," in *Proceedings of the IEEE Conference on Computer Vision and Pattern Recognition*, 2020, pp. 2006–2015.
- [38] S. Lin, R. Ji, C. Yan, B. Zhang, L. Cao, Q. Ye, F. Huang, and D. S. Doermann, "Towards optimal structured CNN pruning via generative adversarial learning," in *Proceedings of the IEEE Conference on Computer Vision and Pattern Recognition*, 2019, pp. 2790–2799.
- [39] M. Alwani, Y. Wang, and V. Madhavan, "DECORE: deep compression with reinforcement learning," in *Proceedings of the IEEE Conference on Computer Vision and Pattern Recognition*, 2022, pp. 12 339–12 349.
- [40] S. Elkerdawy, M. Elhoushi, H. Zhang, and N. Ray, "Fire together wire together: A dynamic pruning approach with self-supervised mask prediction," in *Proceedings of the IEEE Conference on Computer Vision and Pattern Recognition*, 2022, pp. 12 444–12 453.
- [41] S. Xiang, Y. Zhu, X. Shen, and J. Ye, "Optimal exact least squares rank minimization," in *Proceedings of the ACM SIGKDD international conference on Knowledge discovery and data mining*. ACM, 2012, pp. 480–488.
- [42] R. A. Sadek, "Svd based image processing applications: state of the art, contributions and research challenges," *International Journal of Advanced Computer Science and Applications*, vol. 3, no. 7, pp. 26–34, 2012.
- [43] Z. Wang, M. Zoghi, F. Hutter, D. Matheson, and N. de Freitas, "Bayesian optimization in high dimensions via random embeddings," in *Proceedings of the International Joint Conference on Artificial Intelligence*, 2013, pp. 1778–1784.
- [44] F. Tung and G. Mori, "Clip-q: Deep network compression learning by in-parallel pruning-quantization," in *Proceedings of the IEEE conference on computer vision and pattern recognition*, 2018, pp. 7873–7882.
- [45] A. Paszke, S. Gross, F. Massa, A. Lerer, J. Bradbury, G. Chanan, T. Killeen, Z. Lin, N. Gimelshein, L. Antiga, and *et al.*, "Pytorch: An imperative style, high-performance deep learning library," in *Proceedings of the Advances in Neural Information Processing Systems*, 2019, pp. 8024–8035.
- [46] A. Krizhevsky, I. Sutskever, and G. E. Hinton, "Imagenet classification with deep convolutional neural networks," *Communications of the ACM*, vol. 60, no. 6, pp. 84–90, 2017.
- [47] M. D. Zeiler and R. Fergus, "Visualizing and understanding convolutional networks," in *Proceedings of the European Conference on Computer Vision*, vol. 8689, 2014, pp. 818–833.
- [48] Y. Li, S. Lin, J. Liu, Q. Ye, M. Wang, F. Chao, F. Yang, J. Ma, Q. Tian, and R. Ji, "Towards compact cnns via collaborative compression," in *Proceedings of the IEEE Conference on Computer Vision and Pattern Recognition*, 2021, pp. 6438–6447.

VI. PROOF OF THEOREM 1 IN THE PAPER

Proof: Given $\hat{\mathbf{h}} = \mathbf{W}\mathbf{x}$, the gradient $\frac{\partial \mathcal{L}}{\partial \mathbf{x}}$ can be computed

by

$$\frac{\partial \mathcal{L}}{\partial \mathbf{x}} = \mathbf{W}^T \frac{\partial \mathcal{L}}{\partial \hat{\mathbf{h}}}. \quad (12)$$

Since $\mathbb{E}(\frac{\partial \mathcal{L}}{\partial \hat{\mathbf{h}}}) = 0$ and $\text{cov}(\frac{\partial \mathcal{L}}{\partial \hat{\mathbf{h}}}) = \sigma^2 \mathbf{I}$, we have

$$\begin{aligned} \mathbb{E}[(\frac{\partial \mathcal{L}}{\partial \hat{\mathbf{h}}})(\frac{\partial \mathcal{L}}{\partial \hat{\mathbf{h}}})^T] &= \mathbb{E}[(\frac{\partial \mathcal{L}}{\partial \hat{\mathbf{h}}} - \mathbb{E}(\frac{\partial \mathcal{L}}{\partial \hat{\mathbf{h}}}))(\frac{\partial \mathcal{L}}{\partial \hat{\mathbf{h}}} - \mathbb{E}(\frac{\partial \mathcal{L}}{\partial \hat{\mathbf{h}}}))^T] \\ &= \text{cov}(\frac{\partial \mathcal{L}}{\partial \hat{\mathbf{h}}}) = \sigma^2 \mathbf{I}. \end{aligned} \quad (13)$$

The expectation of the square of the gradient norm becomes

$$\begin{aligned} \mathbb{E}(\|\frac{\partial \mathcal{L}}{\partial \mathbf{x}}\|^2) &= \mathbb{E}(\text{tr}(\frac{\partial \mathcal{L}}{\partial \mathbf{x}} \frac{\partial \mathcal{L}}{\partial \mathbf{x}}^T)) \\ &= \mathbb{E}(\text{tr}(\mathbf{W}^T \frac{\partial \mathcal{L}}{\partial \hat{\mathbf{h}}} \frac{\partial \mathcal{L}}{\partial \hat{\mathbf{h}}}^T \mathbf{W})) \\ &= \mathbb{E}(\text{tr}(\frac{\partial \mathcal{L}}{\partial \hat{\mathbf{h}}} \frac{\partial \mathcal{L}}{\partial \hat{\mathbf{h}}}^T \mathbf{W} \mathbf{W}^T)) \\ &= \text{tr}(\mathbb{E}(\frac{\partial \mathcal{L}}{\partial \hat{\mathbf{h}}} \frac{\partial \mathcal{L}}{\partial \hat{\mathbf{h}}}^T) \mathbf{W} \mathbf{W}^T) \\ &= \text{tr}(\mathbb{E}(\frac{\partial \mathcal{L}}{\partial \hat{\mathbf{h}}} \frac{\partial \mathcal{L}}{\partial \hat{\mathbf{h}}}^T) \mathbf{W} \mathbf{W}^T) \\ &= \text{tr}(\sigma^2 \mathbf{W} \mathbf{W}^T) \\ &= \sigma^2 \text{tr}(\mathbf{W} \mathbf{W}^T) \\ &= \sigma^2 \|\mathbf{W}\|_F^2, \end{aligned} \quad (14)$$

where $\text{tr}(\cdot)$ indicates the trace of the corresponding matrix. We use $\mathbb{V}(\cdot)$ to denote the variance of the value. As it is well known, the variance can be represented as follows:

$$\mathbb{V}(\|\frac{\partial \mathcal{L}}{\partial \mathbf{x}}\|) = \mathbb{E}[(\|\frac{\partial \mathcal{L}}{\partial \mathbf{x}}\|)^2] - \mathbb{E}[\|\frac{\partial \mathcal{L}}{\partial \mathbf{x}}\|]^2. \quad (15)$$

Because $\mathbb{V}(\|\frac{\partial \mathcal{L}}{\partial \mathbf{x}}\|) \geq 0$, we have the following relationship for the expectation of the gradient norm

$$\begin{aligned} \mathbb{E}(\|\frac{\partial \mathcal{L}}{\partial \mathbf{x}}\|) &\leq \sqrt{\mathbb{E}[(\|\frac{\partial \mathcal{L}}{\partial \mathbf{x}}\|)^2]} \\ &\leq \sqrt{\sigma^2 \|\mathbf{W}\|_F^2} \\ &\leq \sigma \|\mathbf{W}\|_F. \end{aligned} \quad (16)$$

■